Aerosol and Air Quality Research, 12: 1200–1208, 2012

ISSN: 1680-8584 print / 2071-1409 online
doi: 10.4209/aaqr.2011.11.0198

Micro-Meteorological Elements and Their Vertical Profiles during a Dust Event over a Loess Plateau in March 2010

Xiao-Lu Ling[1], Wei-Dong Guo[1*], Qian-Fei Zhao[2], Ye Liu[1], Jian-Rong Bi[2]

[1] *Institute for Climate and Global Change Research, School of Atmospheric Sciences, Nanjing University, Nanjing 210093, China*
[2] *Key Laboratory for Semi-Arid Climate Change of the Ministry of Education, College of Atmospheric Sciences, Lanzhou University, Lanzhou 730000, China*

ABSTRACT

This research used enhanced observational data of dust concentrations, dynamic factors near the land surface, and vertical distributions of temperature and relative humidity collected from the Semi-Arid Climate and Environment Observatory of Lanzhou University (SACOL), in combination with the NCEP FNL reanalysis data, to study a typical dust event that occurred in Lanzhou during March 2010. The goals are to reveal the background circulation, dynamic factors that caused the dust storm, and vertical profiles of meteorological variables. The results show that this dust event was caused by the interaction of a shortwave trough at high altitude and meso-scale depression system underneath this. Before the dust event, the instability of the low-altitude stratification with the assistance of temperature inversion at higher altitude provided the conditions for strong convection near the surface. During the dust event, the maximum PM_{10} concentration appeared shortly after the maximum wind, and the change in the meridional wind component was bigger than that in the zonal component. The temperature inversion was destroyed at higher altitude, and a significant humidity inversion occurred as a response. Relative humidity gradually decreased with altitude, and the rate of decline increased over time.

Keywords: Dust storm; Vertical distribution; Meteorological elements; Background circulation.

INTRODUCTION

Most arid and semi-arid regions in China are located in the northwest region, of which arid regions account for more than 80% of the total area (Dong *et al.*, 2006). Both observational and numerical modeling studies have shown that an aridity trend is occurring and will become most significantly in the semi-arid region, which is closely related to the life-supporting environment of Chinese people and has been the obstacle of the development of China's national economy (Fu and An, 2002; Fu *et al.*, 2006; Ma and Ren, 2007; Fu and Ma, 2008). According to the statistics, the direct economic loss caused by all kinds of desertification is about 53.49 to 74.89 billion RMB each year, among which the loss to grassland desertification accounts for nearly 12.3% (Zhang *et al.*, 1996; Yang *et al.*, 2006). Furthermore, in all the loss caused by natural disasters, the proportion of the loss caused by meteorological disasters is about 85%, of which the loss caused by drought accounts for about 50% (Obasi, 1994). In particular, economic loss caused by dust storms becomes the most uncertain composition of economical loss assessment due to changing frequency and intensity of dust storms.

Dust aerosols suspended in the air during strong convective weather in arid and semi-arid regions can influence the energy balance by absorbing and scattering shortwave solar radiation and longwave radiation (Qian *et al.*, 1999), which in turn affects major weather processes and short-term climate at local scale. Radiative effects of dust aerosols are mainly cooling the land surface and heating the aerosol layer (Carlson and Benjamin, 1980). According to Tegen *et al.* (1996), dust aerosols can produce about –0.75 W/m^2 of the direct radiative forcing, while its indirect radiative effects can be ignored at the global scale (Prospero and Nees, 1977).

Located at the northern edge of East Asian monsoon region, the semi-arid region of China is characterized by two features: sensitivity to and ability to recover from global environment change (Fu and Ye, 1995; Fu and Wen, 2002; Fu and Guo, 2008). The Loess Plateau, as part of dust aerosol sources, is this kind of semi-arid land surface. To improve our understanding and to collect direct evidence of the impact of human activities on the semi-arid climate over the Loess Plateau, the Semi-Arid Climate and Environment Observatory of Lanzhou University (SACOL)

* Corresponding author. Tel.: +86-25-83592873;
Fax: +86-25-83592873
E-mail address: guowd@nju.edu.cn

was established in the late 2005, which was designed to assess dust aerosol effect on global climate as well as on local climate (Huang *et al.*, 2008). Studies on optical properties of dust aerosols (Fu *et al.*, 2008; Bi *et al.*, 2010; Wang *et al*., 2010), physicochemical characterization (Zhang *et al.*, 2002, 2008; Cao *et al.*, 2009), sources and deposition fluxes (Rastogi *et al.*, 2006; Zhang *et al.*, 2006, 2010), radiative forcing properties (Reddy *et al.*, 2007; Ge *et al.*, 2010; Zhang *et al.*, 2010), measurements of dust aerosol's vertical structure (Huang *et al.*, 2010), remote sensing observations and numerical simulations of dust aerosols (Huang *et al.*, 2007) and dust aerosols' effects on semi-arid climate (Huang *et al.*, 2010) using the first-hand data collected from semi-arid region stations (including the SACOL station) have provided many insightful results. Research on vertical distributions of meteorological elements and dynamic factors, however, is limited, especially on the semi-arid region of China. In this study, the concentration of dust aerosols, vertical distributions of meteorological elements, and dynamic fluxes collected from the SACOL, in combination with the NCEP FNL reanalysis data, are used to analyze the background circulation, dynamic factors, and vertical distributions of meteorological elements during a typical dust event occurred in March 2010.

DATA SOURCES

NCEP Reanalysis Data

The 6-hourly NCEP global reanalysis data with the resolution of 1° × 1° was obtained from the National Center for Atmospheric Research (NCAR). The region of (70°–140°E, 20°–60°N) is used to analyze the background circulation of the dust event in March 2010, while the location of (104°E, 35°N) is taken as the station for the SACOL.

SACOL

The SACOL is actually located at (104.08°E, 35.57°N) in the northwest of the semi-arid region of China, with an annual average precipitation of 381.8 mm. It is situated on the China Loess Plateau, about 1,965.8 m above the sea level. As a climate observation platform based on international standards and in possession of advanced climate and environmental monitoring equipments and instruments as well as a high-quality research team, the SACOL conducts a variety of large-scale field observations. The first-hand data used in this paper are listed as follows.

(1) PM_{10} concentration data came from RP1400a (Thermo, USA), which can continuously sample the aerosols at the height of 3.5 m and record the concentration every five minutes with the units of $\mu g/m^3$.
(2) Dynamic flux was measured at the height of 3.0 m from the eddy covariance system (EC), with a three-axis Sonic Anemometer (CSAT3; Campbell, USA) pointed toward the prevailing wind direction and an open path infrared CO_2 and H_2O analyzer (LI7500 and LI-COR; Campbell, USA) (Wang *et al*., 2010) .
(3) Aerosol vertical distribution (extinction coefficient) was measured using a Micro-Pulse Lidar system (MPL-4; Sigma Space, USA). The MPL has one measurement channel that records backscatter signals up to 20+ km. The primary quantity from this signal is the lowest detected cloud base in meters. Additional quantities, possible through post-processing of the raw signal return, include a relative backscatter profile at 527 nm. Many data products are available from the relative backscatter profile, including multiple cloud decks, cloud and layer boundaries, as well as aerosol extinction and backscatter profiles.
(4) Continuous measurements of temperature and water vapor profiles were carried out with a Radiometrics Profiling Radiometer (TP/WVP-3000; Radiometrics, USA), which produces vertical profiles from the surface to 10 km in height by observing five frequency channels from 22 to 30 GHz and another seven channels from 51 to 59 GHz.

In order to ensure the consistency of the data for analysis, all observational data from the SACOL were averaged over 30-min interval, except for the vertical distributions of meteorological elements.

BACKGROUND CIRCULATIONS

Observed Facts

According to the statistics from the meteorological observatory of Lanzhou, the year 2010 was the year when dust storms occurred most frequently in Lanzhou in the last 30 years. The most serious dust weather occurred on 19 March, when the visibility was only 300 m in the northwest of China, which seriously affected nearly 300 million people in 21 provinces of North, Central, and East China. Fig. 1 shows the daily PM_{10} concentration at the SACOL in March 2010, during which the dust weather days were marked by oblique-lined bars. There was no record of PM_{10} concentration on 19–20 March, due to the bad weather conditions. Except for the missing record on these two days, daily PM_{10} concentration in dust weather days (including dust storm days and dust blowing days) were significantly higher than non-dust days in March, during which the most typical dust process was on 12–14 March, with the daily averaged PM_{10} values of 242.09, 507.44 and 187.83 $\mu g/m^3$. We refer the last two days (13–14 March) as dust storm day and dust blowing day, respectively. Furthermore, the day on 15 March with the PM_{10} value of 52.48 $\mu g/m^3$ is treated as sunny day for comparison.

Background Circulation

Fig. 2 shows the circulations at 850 and 500 hPa at 1200 LST on 13 March 2010. It can be seen that the geographic center of this dust event was situated in front of the high-altitude shortwave through (Fig. 2(a)). At 500 hPa, the area from western Mongolia to Xinjiang Uyghur Autonomous Region (in Northwest China) was controlled by a low pressure system, with the interaction of shortwave trough in the direction from northeast to southwest and the cold center of temperature at –40°C over western Mongolia where there was prevailing west-northwesterly air stream. The trough was strengthened and the stability of the atmospheric layer was

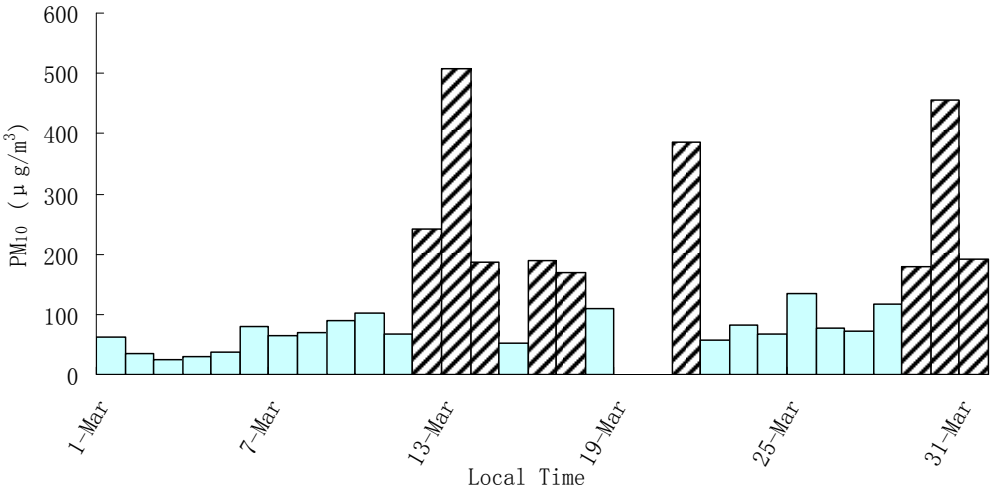

Fig. 1. Daily PM_{10} concentration at the SACOL in March 2010.

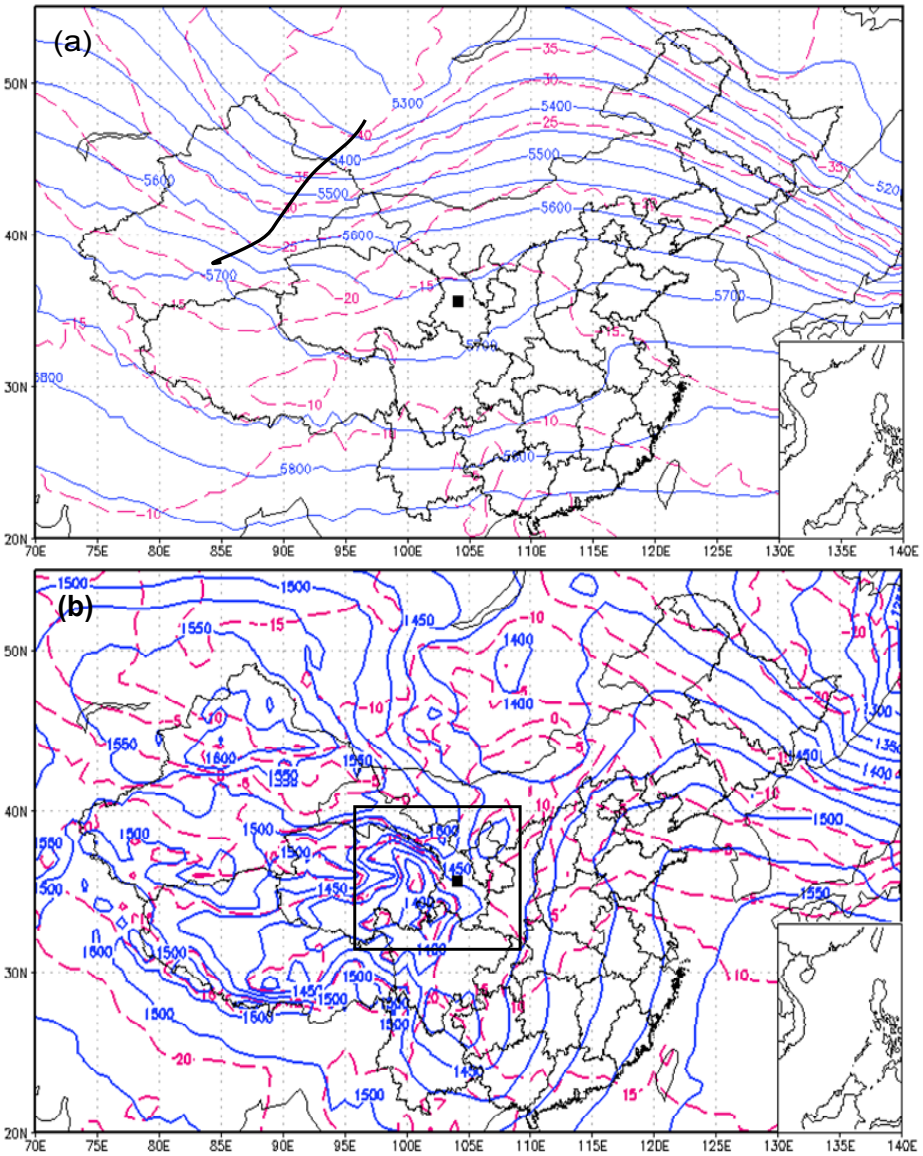

Fig. 2. Spatial distribution of geopotential height and temperature circulations at 1200 LST on 13 March 2010 ■ at SACOL: (a) 500 hPa and (b) 850 hPa.

reduced, a situation that stimulated the development of strong convection and provided impetus for a dust process.

The lower layer (Fig. 2(b)) had a matching feature of meso-scale circulation to the upper layer. There was a strong depression centered around (100°E, 35°N) near the front of the upper-layer shortwave trough, and the isobars and isotherms in the direction from northwest to southeast were very closely packed, indicating the cold air invaded into the northeast and increased the horizontal temperature gradient, which was beneficial for front genesis near the surface. Accordingly, a significant meso-scale depression center was formed near the middle of Gansu Province, resulting in strong cyclonic convergence and strengthening upward air movement in low altitude. Therefore, the interaction of shortwave trough at high altitude and meso-scale depression resulted in cyclonic shear and convergence updraft, which provided impetus for the occurrence of a dust event.

Backward Trajectory Analyses

We calculate the 72-hour mass back trajectories at 500 m above the ground of the SACOL at 0000 LST on 15 March 2010 using the NOAA Hybrid Single Particle Lagrangian Integrated Trajectory Model (HYSPLIT-4) to investigate the soil dust transport pathway. HYSPLIT-4 is a complete system for computing trajectories in complex dispersion and deposition simulations using either puff or particle approaches developed by the US NOAA/Air Resources Laboratory and the Australian Bureau of Meteorology (Yin *et al*., 2007; Cao *et al*., 2009). For detailed instruction, readers are referred to the User's Guide (Draxler and Hess, 1997). With the source at the 500-m level over the SACOL, using 2.5° × 2.5° NCEP FNL reanalysis data (http://ready.arl.noaa.gov/archives.php) from 0000 LST on 15 March 2010 backtrack to 0000 LST on 12 March, the total integral time is 72 hours and each aerosol particle was released every 6 hours. The results show that the air mass came from the northwest air stream at high altitude, and dust particles were transported a long distant before their arrival at the SACOL. Analysis of the vertical dust particles' profiles during transmission (not shown) revealed that dust particles were distributed in the near-surface layer from 0000 LST on 15 March back tracked to 13 March while at the high altitude of about 2 km back tracked to 12 March, indicating that long-range transportation of dust particles happened at a higher altitude.

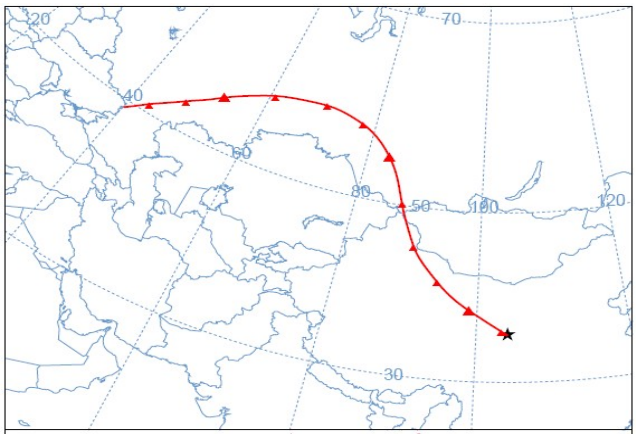

Fig. 3. Backward trajectories ending at the SACOL at 0000 LST on 15 March 2010.

DYNAMIC FACTORS NEAR LAND SURFACE

Fig. 4 shows the variation of dynamic factors at the SACOL during 13–15 March 2010, which is used to analyze the features of horizontal wind and vertical velocity. It can been seen in Fig. 4(a) that the vertical velocities had significant differences on the dust storm day, dust blowing day, and sunny day, in which the most intensely changing period was from 1630 LST to 2130 LST on 13 March 2010, which corresponds to the maximum PM_{10} concentration and therefore indicates the very relationship of rapid change of vertical speed in a short period and the amount of dust particles. Fig. 4(b) shows the changes of horizontal wind components over time, namely, the U component had the same change as the V component, and both had the same trend as the vertical velocity. Both U and V components reached their maxima at about 1900 LST, and then followed the largest concentration of PM_{10}, with the change amplitude of V component being slightly larger than that of U. Fig. 4(c) describes the relationship of vertical velocity, horizontal wind components, and dust concentration. During this dust storm event, when the V component and vertical velocity showed a significant negative relationship, dust concentration reached its maximum. This relationship could be interpreted as follows. If the upward vertical movement strengthened or downward movement weakened, the corresponding situation beneficial for the uplifting of dust particles was the strengthening of westward flow or northward flow. If the upward vertical movement weakened or downward movement strengthened, the corresponding situation beneficial for the accumulation of dust particles is the weakening of westward flow or northward flow. So, we can conclude that the rising of dust particles is the result of both vertical velocity and horizontal wind components.

Above all, before the dust event on 13 March the vertical velocity was downward and strengthened, the northward and westward wind components were wave-like and strengthened, which made dust particles from the northwest subside from an upper layer and provided a good dust source for this dust storm event. With the vertical movement changed gradually to upward and became stronger, the covariance of vertical velocity and horizontal wind components changed acutely accordingly. Due to the combination of cyclonic shear and upward movement, dust particles near the land surface were rolling up and caused this dust storm event.

VERTICAL DISTRIBUTIONS OF METEOROLOGICAL ELEMENTS

Fig. 5 displays the variation of backscatter intensity of the MPL at the SACOL on 13 March 2010. The white areas represent the particles with backscattering coefficient larger than 0.26 that are considered as clouds, the green and orange

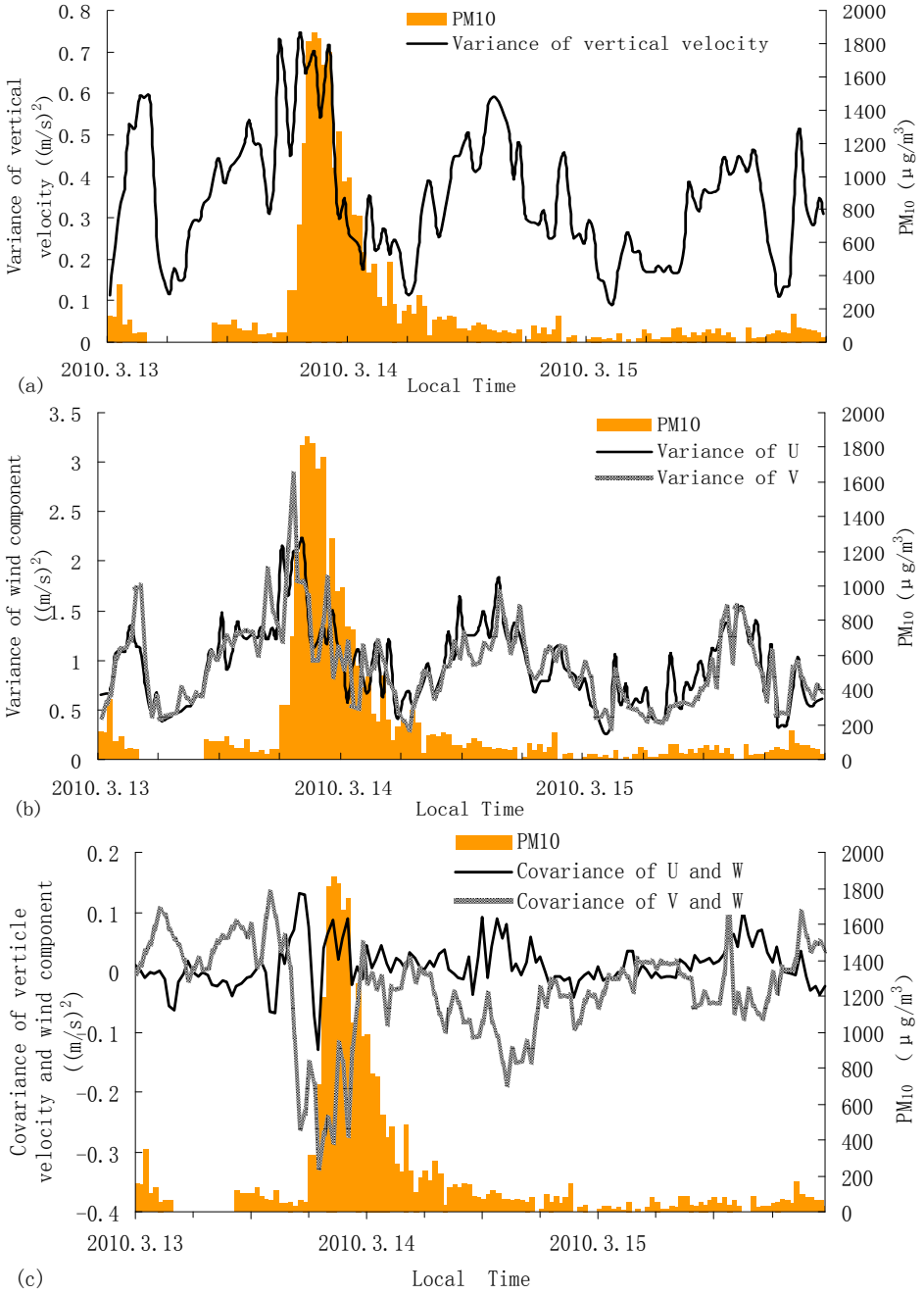

Fig. 4. Variation of dynamic factors at the SACOL during 13–15 March 2010: (a) variance of vertical velocity; (b) variance of horizontal wind components; and (c) covariance of vertical velocity and horizontal wind components.

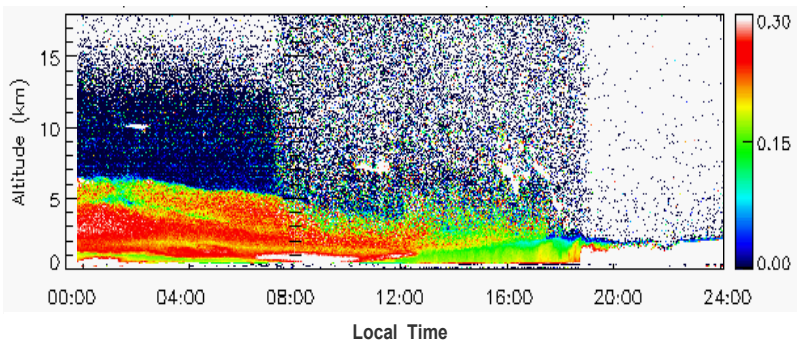

Fig. 5. Micro-Pulse Lidar backscatter intensity at the SACOL on 13 March 2010.

colors represent the particles with backscattering coefficient between 0.1 and 0.25 that are generally believed to be aerosols, and the blue colors are for the backscattering coefficient less than 0.1 that are considered as gas molecules. By analyzing Fig. 5, we can see that from 0000 to 0800 LST on 13 March, a large number of coarse particles were gathering between 1 and 5 km over the SACOL. Afterward, the thickness of coarse particles gradually thinned, and at 1200 LST coarse particles were concentrated over the altitude range from 0.5 to 3 km. After the coarse particles subsided gradually, a large number of dust aerosols suspended in the atmosphere from near-surface to the height of 3 km; the situation was recorded by the observatory station as dust flowing day and last until 1830 LST, followed by the ground dust aerosols that quickly rolled up by high wind and formed dust storm from 1900 to 2400 LST. It is worth noting that although large dust concentration near the land surface and terrible weather conditions interrupted the measuring of backscattering intensity of the MPL to a certain degree, the changes seen in Fig. 5 are consistent with those in Fig. 4; so, it is useful to analyze the changes of meteorological elements associated with the dust aerosols in terms of their vertical distributions.

Fig. 6 displays the vertical distributions of meteorological factors (including temperature and relative humidity) during the dust and non-dust days, with the time interval of 3 hours. During the dust day from 0000 to 0300 LST, the temperature profile from the near-surface to 700-m height displayed the situation of neutral stratification, indicating the presence of strong turbulence. As time went by, the temperature near the land surface increased faster than the temperature above because of the solar radiation, the lapse rate at lower altitude decreased quickly but increased at a higher altitude, which formed an inflection point at 300 m. The situation of strong adiabatic lapse rate below 300 m and temperature inversion between 300 and 600 m sustained and became most obviously during 0900–1200 LST, resulting in strong wind in the lower altitude that made dust aerosols roll up and down in the atmosphere and stable air stratification at the higher altitude and caused dust aerosols to accumulate and suspend in the atmosphere. After 1200 LST, the higher altitude temperature inversion disappeared, and the whole atmosphere below 1 km became unstable, which was accompanied by strong convection and large wind velocity, providing a favorable condition for the occurrence of this dust event. While for the non-dust day, the changes of vertical temperature distribution during the whole day were very gentle. During the peak time of PM_{10} concentration, the temperature lapse rate increased rapidly, which were –8.0, –6.1 and –6.2 K/km for 1800, 2100 and 2400 LST, respectively. While on the non-dust day, the lapse rate were only –7.3, –2.2 and –2.4 K/km, respectively.

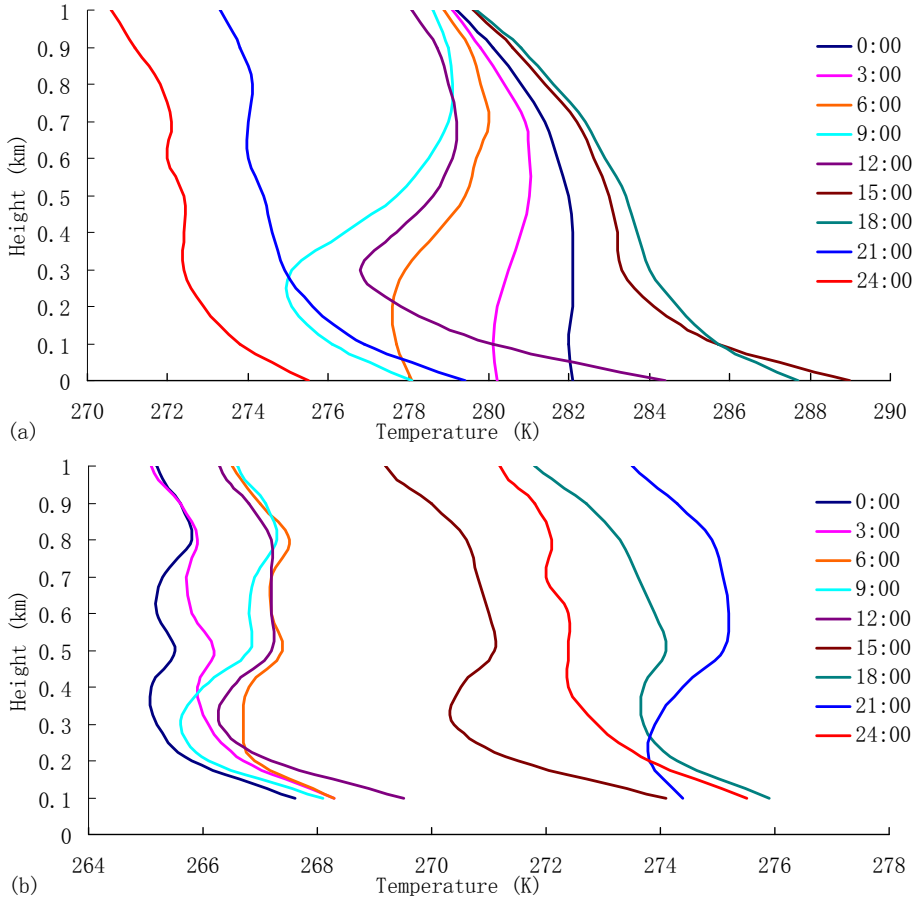

Fig. 6. Vertical distributions of meteorological elements on 13 March and 15 March 2010: vertical temperature distribution on (a) dust day and (b) non-dust day; and vertical relative humidity distribution on (c) dust day and (d) non-dust day.

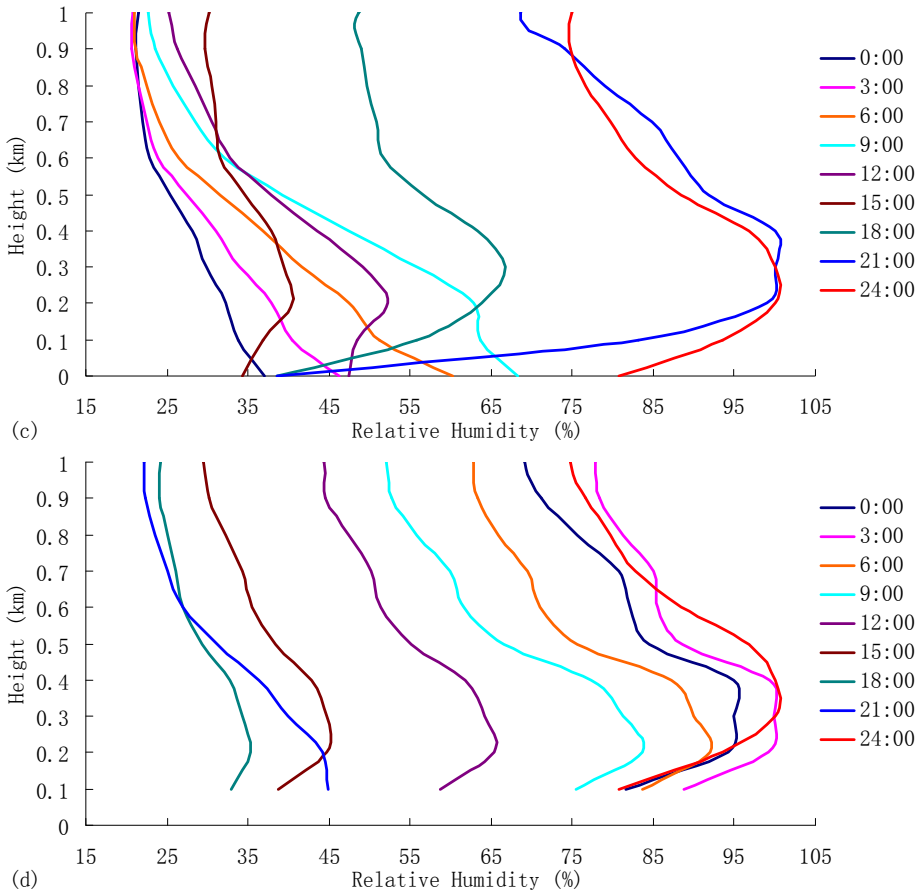

Fig. 6. *(continued).*

In the meantime, the relative humidity responded more significantly with altitude than temperature during the dust sedimentation: the relative humidity decreased with altitude from 0000 to 0900 LST and the decline rate became larger over time (Fig. 6(c)). Since the decline rate was far greater over 200 m than below, there was a weak inflection point at 200 m. From 0900 LST, the inflection point became more significant and moved up to about 300 m; the vertical profile of relative humidity gradually changed into neutral, and the relative humidity even increased quickly from the near-surface to the inflection layer, though the relative humidity still decreased with altitude where it was higher than 300 m. The relative humidity reached its daily minimum at 1500 LST, when the relative humidity below 1 km only changed in the range from 30% to 40%. Followed by the relative humidity increase with altitude quickly, the situation sustained until 0000 LST of 14 March, with the maximum at 2100 LST on 13 March. For the non-dust day, the vertical distribution of relative humidity changed little (Fig. 6(d)). Take the rapid increase time in PM_{10} concentration recorded by the ground observatory as an example, the relative humidity changed from 38.6% near the ground to 100.0% at about 300 m on the dust day, but only from 45.7% to 40.0% on the non-dust day.

Fig. 7 displayed the vertical distributions of V wind component and vertical velocity at 1200 LST on the dust and non-dust days, respectively. During the dust event, the northward wind prevailed over the SACOL, while on the non-dust day a strong southward jet lay on the 400-hPa geopotential height field, and the wind gradually spread downward to the 750-hPa level (Fig. 7(a)). In Fig. 7(b), the negative vertical velocity indicates the prevailing of updraft on the dust day, making it obvious that this dust storm event was the product of upward movement.

CONCLUSIONS AND DISCUSSIONS

We used the observational data of dust concentration, dynamic fluxes, vertical profiles of temperature and relative humidity collected at the SACOL, in combination with the NCEP FNL reanalysis data, to analyze the background circulation, dynamic conditions, and vertical meteorological elements during a typical dust event in Lanzhou in March 2010. The results are as follows.

(1) This dust storm event resulted from cyclonic shear and convergent updraft, which were caused by the interaction of shortwave trough at high altitude and meso-scale depression system underneath. The dust particles were transported over a long distant to the SACOL by the air mass passed from northwest air stream at a high altitude.

(2) The uplifting of dust particles resulted from the interaction of horizontal wind and vertical velocity, in which the rapid change of vertical velocity over a short

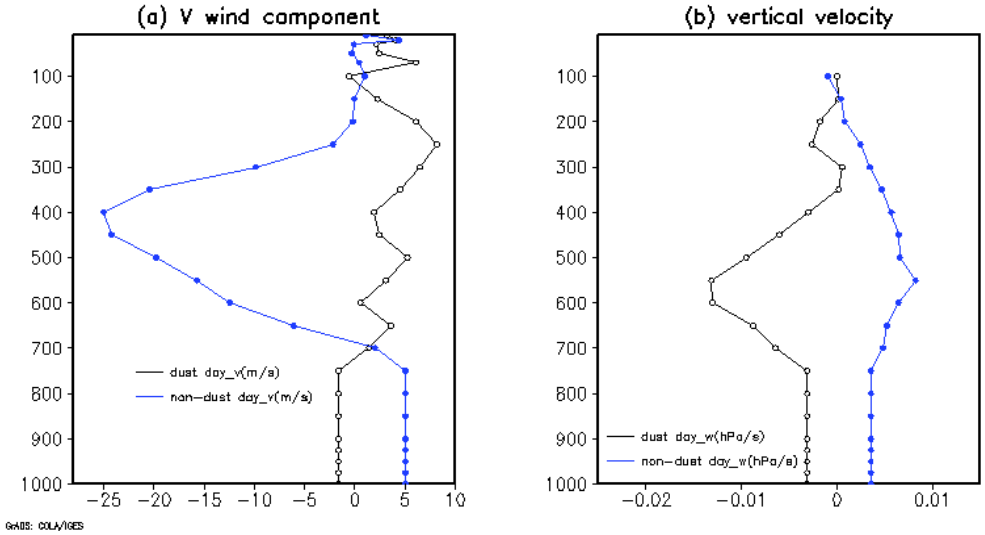

Fig. 7. Vertical distributions of (a) V wind component and (b) vertical velocity on 13 March and 15 March 2010.

time and the change of dust concentration occurred nearly at the same time. Furthermore, the maximum PM_{10} concentration occurred shortly after the maximum horizontal wind components, and the change in the V component was larger than that in U.

(3) The instability of low-altitude stratification with the assistance of temperature inversion at a higher altitude provided an advantage for the strong convection near the surface before this dust event started. Relative humidity responded more significantly during the dust sedimentation: it decreased with altitude gradually and its lapse rate increased over time. During the dust event, the temperature inversion was destroyed at the high altitude, and an obvious humidity inversion occurred as a response.

We tried to analyze the interaction of dust aerosols and semi-arid region in terms of dynamics and large-scale background circulation, and achieved some meaningful results. In our future study, we will include more dust events use remote sensing satellite data, and perform quantitative analysis on vertical distribution of dust aerosols.

ACKNOWLEDGEMENTS

We are grateful for the excellent data and supports provided by the people at SACOL, Lanzhou University. The NCEP global reanalysis data was obtained from the National Center for Atmospheric Research (NCAR) data management center website. This study is jointly supported by the National Basic Research Program of China (grant Nos. 2010CB428503 and 2011CB952002), the National Natural Science Foundation of China (grant Nos. 40975049 and 40810059003), and by a project funded by the Priority Academic Program Development of Jiangsu Higher Education Institutions.

REFERENCES

Bi, J.R., Huang, J.P., Fu, Q., Wang, X., Shi, J.S., Zhang, W., Huang, Z.W. and Zhang, B.D. (2010). Toward Characterization of the Aerosol Optical Properties over Loess Plateau of Northwestern China. *J. Quant. Spectrosc. Radiat. Transfer* 112: D00K17, doi: 10.1029/2009JD01 3372.

Cao, J.J., Zhang, T., Chow, J.C., Waston, J.G., Wu, F. and Li, H. (2009) Characterization of Atmospheric Ammonia over Xi'an, China. *Aerosol Air Qual. Res.* 9: 277–289.

Cao, X.J., Zhang, L., Zhou, B., Bao, J., Shi, J.S. and Bi, J.R. (2009). Lidar Measurement of Dust Aerosol Radiative Property over Lanzhou. *Plateau Meteorol.* 28: 1115–1120.

Carlson, T.N. and Benjamin, S.G. (1980). Radiative Heating Rates for Saharan Dust. *J. Atmos. Sci.* 37: 193–213.

Dong, A.X., Bai, H.Z. and Lei, X.B. (2006). New Development of Arid Climate Research in Northwest China from 2001 to 2005 and Main Scientific Problems. *Arid Meteorol.* 24: 57–62.

Draxler, R.R. and Hess, G.D. (1997). *Description of the Hysplit_4 Modeling System*, NOAA Technical Memorandum ERL ARL, p. 224.

Fu, C.B. and Ye, D.Z. (1995). Global Change and the Future Trend of Ecological Environment Evolution in China. *Sci. Atmos. Sin.* 19: 116–126.

Fu, C.B. and An, Z.S. (2002). Study of Aridification in Northern China–A Global Chance Issue Facing Directly the Demand of Nation. *Earth Sci. Front*. 9: 271–275.

Fu, C.B. and Wen, G. (2002). Several Issues on Aridification in the Northern China. *Clim. Environ. Res.* 7: 22–29.

Fu, C.B., Yan, X.D. and Guo, W.D. (2006). Aridification in the Northern China and Human Adaptation. *Prog. Nat. Sci.* 16: 1216–1223.

Fu, C.B. and Guo, W.D. (2008). *Regional Climate of China, Chap. 5: Aridity Trend in Northern China*, Springer Publishing House, p. 155–217.

Fu, C.B. and Ma, Z.G. (2008). Global Change and Regional Aridification. *Chin. J. Atmos. Sci.* 32: 752–760.

Fu, P.J., Huang, J.P., Li, C.W. and Zhong, S.R. (2008). The Properties of Dust Aerosol and Reducing Tendency of the Dust Storms in Northwest China. *Atmos. Environ.*

42: 5896–5904.

Ge, J.M., Su, J., Ackerman, T.P. Fu, Q., Huang, J P. and Shi, J.S. (2010). Dust Aerosol Optical Properties Retrieval and Radiative Forcing over northwestern China during the 2008 China-U.S Joint Field Experiment. *J. Geophys. Res.* 115: D00K12, doi: 10.1029/2009JD013263.

Huang, J.P. , Zhang, W., Zuo, J.Q., Bi, J.R., Shi, J.S., Wang, X., Chang, Z.L., Huang, Z.W., Yang, S., Zhang, B.D., Wang, G.Y., Feng, G.H., Yuan, J.Y., Zhang, L., Zuo, H.C., Wang, S.G., Fu, C.B. and Chou, J.F. (2008). An Overview of the Semi-arid Climate and Environment Research Observatory over the Loess Plateau. *Adv. Atmos. Sci.* 25: 906–921.

Huang, J.P., Ge, J.M. and Weng, F. (2007). Detection of Asia Dust Storms Using Multisensor Satellite Measurements. *Remote Sens. Environ.* 110: 186–191.

Huang, J.P., Minnis, P., Yan, H.R., Yi, Y., Chen, B., Zhang, L. and Ayers, J.K. (2010). Dust Aerosol Effect on Semi-arid Climate over Northwest China Detected from A-Train Satellite Measurements. *Atmos. Chem. Phys.* 10: 6863–6872.

Huang, Z.W., Huang, J.P., Bi, J.R., Wang, G.Y., Wang, W.C., Fu, Q., Li, Z.Q., Tsay, S.C. and Shi, J.S. (2010). Dust Aerosol Vertical Structure Measurements Using Three MPL Lidars during 2008 China-U.S. Joint Dust Field Experiment. *J. Geophys. Res.* 115: D00K15, doi: 10.1029/2009JD013273.

Ma, Z.G. and Ren, X.B. (2007). Drying Trend over China from 1951 to 2006. *Adv. Clim. Change Res*. 3:195–200.

Obasi, G. (1994). WMO's Role in the International Decade for Natural Disaster Education. *Bull. Am. Meteorol. Soc.* 75:1655–1661.

Prospero, J.M. and Nees, R.T. (1977). Dust Concentration in the Atmosphere of the Equatorial North Atlantic: Possible Relationship to the Sahelian Drought. *Science* 196: 1196–1198.

Qian, Y., Fu, C.B. and Wang, S.Y. (1999). Mineral Dust and Climate Change. *Adv. Earth Sci*. 14: 391–394.

Rastogi, N. and Sarin, M. (2006) Atmospheric Abundances of Nitrogen Species in Rain and Aerosols Over a Semi-arid Region: Sources and Deposition Fluxes. *Aerosol Air Qual. Res*. 6: 406–417.

Reddy, R.R., Gopal, K.R., Narasimhulu, K., Reddy, L.S.S. and Kumar, K.R. (2007) Aerosol Size Distribution Variation in Anantapur (14.62°N, 77.62°E) Semi Arid Zone and its Impact on Aerosol Effective Radius. *Aerosol Air Qual. Res.* 7: 550–562.

Tegen, I, Lacis, A.A. and Fung, I. (1996). The influence on Climate Forcing Mineral Aerosols from Disturbed Soils. *Nature* 380: 419–422.

Wang, G.Y., Huang, J.P., Guo, W.D., Zuo, J.Q., Wang, J.M., Bi, J.R., Huang, Z.W. and Shi, J.S. (2010). Observation Analysis of Land-atmosphere Interactions over the Loess Plateau of Northwest China. *J. Geophys. Res.* 115: DOOK17, doi: 10.1029/2009JD013372.

Wang, X., Huang, J.P., Zhang, R.D., Chen, B. and Bi, J.R. (2010). Surface Measurements of Aerosol Properties over Northwest China during ARM China 2008 Deployment. *J. Geophys. Res.* 115: D00K27, doi: 10.1029/2009JD013467.

Yang, J.J., Zhang, K.B., Qiao, F. and Li, R. (2006). The Research Course in Study of Economic Loss of Desertification. *Res. Soil Water Conserv*. 13: 40–43.

Yin, X.H., Shi, S.Y., Zhang, M.Y. and Li, J. (2007). Change Characteristic of Beijing Dust Weather and Its Sand-Dust Source Areas. *Plateau Meteorol*. 26: 1039–1044.

Zhang, L., Cao, X.J., Bao, J., Zhou, B., Huang, J.P., Shi, J.S. and Bi, J.R. (2010). A Case Study of Dust Aerosol Radiative Properties over Lanzhou, China. *Atmos. Chem. Phys*. 10: 4283–4293.

Zhang, R.J., Arimoto, R., An, J.L., Yabuki, S., Sun, J.H. (2005). Ground Observations of a Strong Dust Storm in Beijing in March 2002. *J. Geophys. Res.* 110: D18S06, doi: 10.1029/2004JD004 589.

Zhang, R.J., Wang, Z.F., Shen, Z.X., Yabuki, S., Kanai, Y. and Ohta, A. (2006). Physicochemical Characterization and Origin of the 20 March 2002 Heavy Dust Storm in Beijing. *Aerosol Air Qual. Res.* 6: 268–280.

Zhang, R.J., Han, Z.W., Shen, Z.X. and Cao, J.J. (2008). Continuous Measurement of Number Concentrations and Elemental Composition of Aerosol Particles for a Dust Storm Event in Beijing *Adv. Atmos. Sci.* 25: 89–95.

Zhang, R.J., Shen, Z.X., Cheng, T.T., Zhang, M.G. and Liu, Y.J. (2010). The Elemental Composition of Atmospheric Particles at Beijing during Asian Dust Events in Spring 2004. *Aerosol Air Qual. Res.* 10: 67–75.

Zhang, Y., Ning, D.T. and Vaclav, S. (1996). An Estimate of Economic Loss for Desertification in China. *China Population, Resour. Environ.* 6: 45–48.

Received for review, November 11, 2011
Accepted, February 24, 2012